Spirotetrahydroisoquinoline-Based Histone Deacetylase Inhibitors as New Antifibrotic Agents: Biological Evaluation in Human Fibroblasts from Bronchoalveolar Lavages of Idiopathic Pulmonary Fibrosis Patients

Spirotetrahydroisoquinoline-based histone deacetylase inhibitors as new anti-fibrotic agents: biological evaluation in human fibroblasts from bronchoalveolar lavages of idiopathic pulmonary fibrosis patients

Anna Fontana[γ], Laura Bergantini[ε], Gabriele Carullo[γ], Laura Scalvini[φ], Miriana D'Alessandro[ε], Chiara Papulino[ω], Paolo Cameli[ε], Sara Gangi[ε], Fabrizio Vincenzi[§], Katia Varani[§], Chiara Contri[§], Silvia Pasquini[θ], Anna Pistocchi[ψ], Alex Pezzotta[ψ], Sabrina Carbone[ψ], Simona Saponara[μ], Sandra Gemma[γ,*], Lucia Altucci[ω,Θ,ϱ], Rosaria Benedetti[ω], Alessio Lodola[φ], Marco Mor[φ,ζ], Elena Bargagli[ε], Stefania Butini[γ], Giuseppe Campiani[γ,*]

[γ]Department of Biotechnology, Chemistry and Pharmacy, University of Siena, Via Aldo Moro 2, 53100 Siena, Italy.

[ε]Department of Medical Science, Surgery and Neuroscience, University of Siena, Policlinico Santa Maria alle Scotte, Viale Mario Bracci 16, 53100 Siena, Italy.

[φ]Department of Food and Drug, University of Parma, 43124 Parma, Italy.

[ω]Department of Precision Medicine, University of Campania Luigi Vanvitelli, 80138 Naples, Italy.

[§]Department of Translational Medicine, University of Ferrara, 44121 Ferrara, Italy.

[θ]Department of Chemical, Pharmaceutical and Agricultural Sciences, University of Ferrara, 44121 Ferrara, Italy.

[ψ]Department of Medical Biotechnology and Translational Medicine, University of Milan, 20054 Segrate (Milan), Italy.

[μ]Department of Life Sciences, University of Siena, Via Aldo Moro 2, 53100 Siena, Italy.

[Θ] Biogem Institute of Molecular and Genetic Biology, 83031Ariano Irpino (Avellino), Italy.

[ϱ] Institute of Endocrinology and Oncology "Gaetano Salvatore" (IEOS), 80131 Naples, Italy.

[ζ] Microbiome Research Hub, University of Parma, Parma, Italy

Abstract

Idiopathic pulmonary fibrosis (IPF) is a rare interstitial lung disease typified by a progressive-fibrosing phenotype. IPF has been associated with an aberrant HDAC activity, particularly HDAC6. Combining synthetic and modelling studies, a new family of spirotetrahydroisoquinoline-capped histone deacetylase inhibitors **5a-o** was developed. These analogues were prepared via the three-component Castagnoli-Cushman reaction (CCR) as the key step. Structure-activity relationship (SAR) studies identified **5n** as a preferential HDAC6 inhibitor, with a suitable degree of selectivity compared to HDAC1, HDAC3, HDAC5, HDAC8, HDAC10 and HDAC11. **5n** was able to negatively modulate the expression of fibrotic markers fibronectin and collagen 1 in fibroblasts deriving from bronchoalveolar lavages of IPF patients. In another ex vivo IPF human model, **5n** reduced the expression of fibronectin and negatively affected the expression of collagen 1 and vimentin, this latter associated with invasiveness. Finally, **5n** did not show toxicity rat-perfused heart and zebrafish larvae.

KEYWORDS: *histone deacetylase, HDAC6, Castagnoli-Cushman reaction, idiopathic pulmonary fibrosis, IPF, BAL*.

List of Abbreviations

ABCs, airway basal cells; BAL, bronchoalveolar lavage; IPF, idiopathic pulmonary fibrosis; CCR, Castagnoli-Cushman reaction; DCM, dichloromethane; DMF, *N*,*N*-dimethylformamide; DMSO, dimethyl sulfoxide; ECM, extracellular matrix; ESI-MS, electrospray ionization mass spectrometry; EtOAc, ethyl acetate; H_2, molecular hydrogen; HCl, hydrochloric acid HDAC, histone deacetylase; HDACi, histone deacetylase inhibitor; H_2O, water; Hsp90, heat shock proteins 90; HLF, human lung fibroblasts; HPLC, high-performance liquid chromatography; HRMS, high-resolution mass spectrometry; K_2CO_3, potassium carbonate; KOH, potassium hydroxide; LCMS, liquid chromatography−mass spectrometry; $LiAlH_4$, lithium aluminum hydride; MD, molecular dynamics; MeCN, acetonitrile; MeOH methanol; N_2, molecular nitrogen; NAD, nicotinamide adenine dinucleotide; Na_2SO_4, sodium sulfate; NH_2OAc, ammonium acetate; NH_2OH, hydroxylamine; NH_4OH, ammonium hydroxide; Pd/C, palladium on carbon; PE, petroleum ether; r.t., room temperature; α-SMA, α-smooth muscle actin; SAR, structure-activity relationship; SI, selectivity index; TEA, triethylamine; TFA, trifluoroacetic acid; TGF-β1, transforming growth factor β1; THF, tetrahydrofuran; THIQ, tetrahydroisoquinoline; TLC, thin-layer chromatography; UV, ultraviolet; ZBG, zinc-binding group.

Among the rare diseases, idiopathic pulmonary fibrosis (IPF) is one of the most debilitating and life-threatening, being a chronic, degenerative, and fibrotic interstitial lung disorder of unknown etiology, and with an unpredictable prognosis.[1,2]

IPF is characterized by a progressive replacement of the lung parenchyma with fibrous connective tissue. Dysregulations of the injury repair might be due to diverse phenotypic changes including the activation of fibroblasts into activated myofibroblasts, and lung parenchyma epithelial-mesenchymal transition (EMT), a transforming growth factor (TGF-β1)-mediated process that enables the epithelial cells to take on a mesenchymal phenotype.[3,4]

The pool of differentiated cells, further enriched by the airway basal cells (ABCs), can migrate in the lung interstitium forming the fibrotic foci, specific agglomerates responsible for the overaccumulation of extracellular matrix (ECM) components, such as collagen types I and III, fibronectin, vimentin and other proteins. Collectively, these events compromise the gas exchange at the alveolar level with consequent impairment of respiratory function.[5]

As for other rare diseases, treatment of IPF still relies on a few therapeutic options that are not resolutive.[6] Accordingly, the currently recommended therapy includes pirfenidone (Esbriet®), and nintedanib (Ofev®) which contribute to relieve symptoms and delay the disease progression with manageable collateral effects. Nevertheless, both drugs are unable to eradicate the disorder, and to date lung transplantation often represents the resolutive option.[7,8]

The paucity of reliable disease models is prioritizing the discovery of innovative approaches to both investigate IPF pathogenesis and validate new druggable targets.[5,9]

In recent years the proteomic analysis of bronchoalveolar lavage (BAL) fluid provided many insights concerning the major profibrotic mediators, enabling the study of IPF at a molecular level.[10–12] Fibroblasts derived from BAL fluid constitute an innovative IPF investigation model.[12] Concerning the targets under scrutiny for IPF, histone deacetylases (HDACs) were proved to participate in IPF-related fibrogenesis by contributing to profibrotic pathways thanks to the SMAD family member 3/TGF-β axis.[13]

HDAC enzymes catalyze the cleavage of the acetyl groups from *N*-acetyl lysine residues on histones, serving as epigenetic modulators, and other non-histone proteins like cortactin, α-tubulin, heat shock protein 90 (Hsp90). The 18 human HDACs are classified into two groups, based on the presence of a zinc atom in the active site. The Zn^{2+}-dependent enzymes are in turn clustered into: *i)* class I, the truly epigenetic enzymes HDAC1, 2, 3 and 8 preferentially located in the nucleus; *ii)* class IIa (HDAC4, 5, 7, 9), still unexplored enzymes and with a limited physiological significance; *iii)* class IIb, including HDAC6 and 10, enzymes with a prevalent cytoplasmic localization; *iv)* class IV (HDAC11) with a limited interest. The other enzymes are NAD^+-dependent enzymes, representing the class III of HDACs, also known as sirtuins (SIRT1-7).[14]

Among the subtypes, HDAC6 exhibits distinctive features based on its structure, major cytoplasmatic localization, substrate repertoire, and biological functions.[15] Unlike the other HDACs, HDAC6 exclusively contains a zinc-finger ubiquitin-binding domain, and two independent catalytic domains, namely CD1 and CD2, of which only the latter has been speculated to be primarily responsible for the deacetylase activity.[16] While retaining a limited epigenetic activity, HDAC6 predominantly operates on a broad pool of non-histone substrates, such as α-tubulin, cortactin, Hsp90 and peroxiredoxin.[17,18]

Myofibroblasts of IPF tissues generally show an activation and atypical upregulation of class I and class II HDACs, as well as aberrant bronchiolar epithelium, whereas alveolar epithelial cells show a significant depletion of many HDACs.[13] In this context, selective inhibitors of both class I[19] and class II[20] demonstrated efficacy in reversing IPF phenotype.

HDAC6 enzyme is particularly upregulated in multiple disorders, and over the years several small-molecule inhibitors were developed to antagonize its aberrant activity.[3,14] Many endeavors were addressed to attain HDAC6 preferential binding, culminating in the development of selective inhibitors like compounds **1**-**4** (**Figure 1**).[21–24] Our recent research revealed a strong correlation between HDAC6 overexpression and apoptosis resistance in ABCs derived from IPF patients.[25]

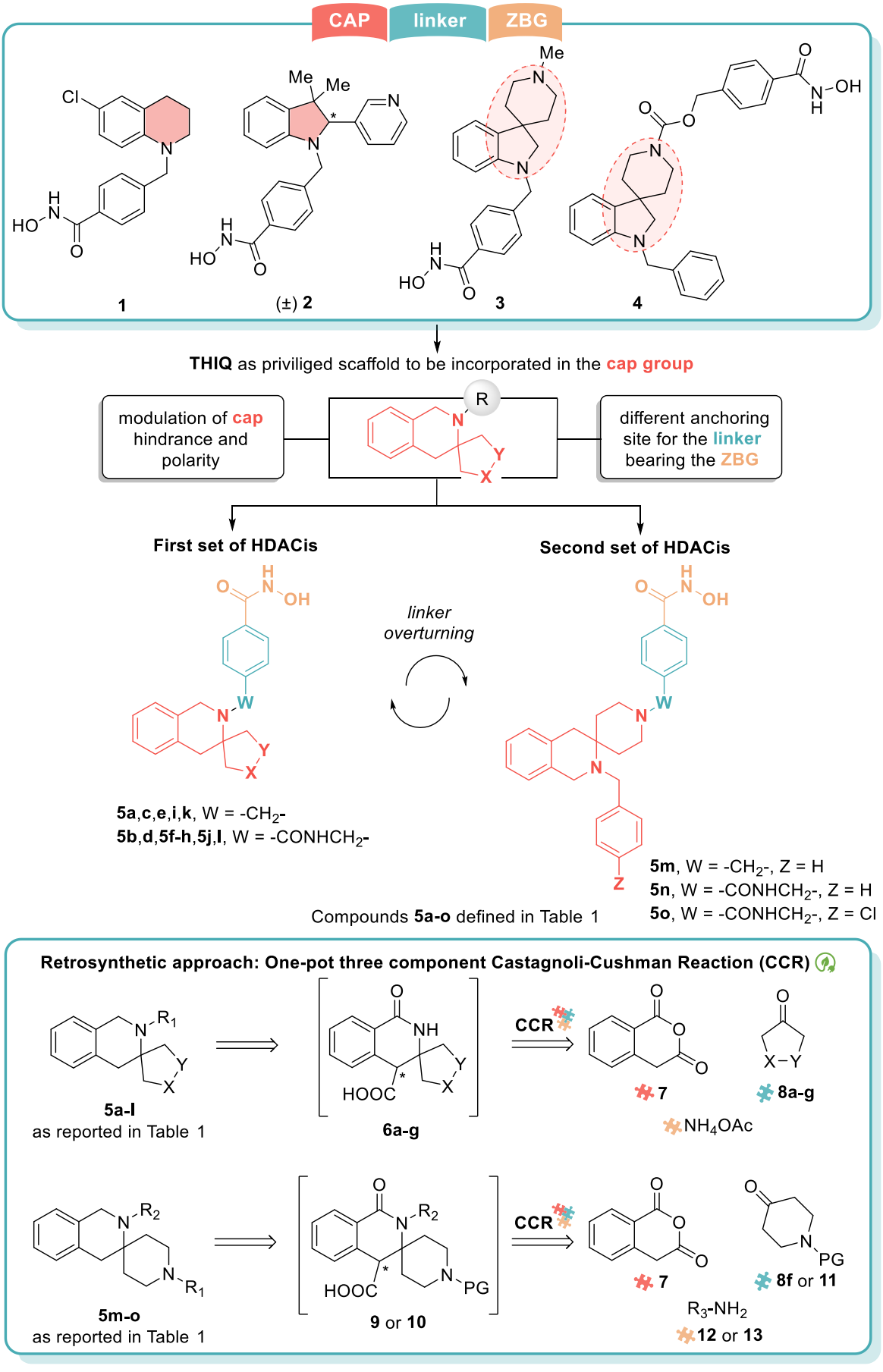

Figure 1. Design of HDAC6is **5a-o** based on a structural analysis of known selective inhibitors and retrosynthetic approaches based on CCR.

Differently decorated HDAC6 inhibitors,[20,26] but also other HDAC inhibitors targeting HDAC1[19] and HDAC8[27] have been proposed as potential anti-fibrotic agents, with in vitro and in vivo efficacy. We previously validated the spiroindoline-based HDAC6i **2** (**Figure 1**), as effective in reverting the IPF phenotype, by inhibiting the fibrotic sphere formation in a 3D cell model derived from patient ABCs.[25] Despite efficacy, the chiral nature of **2** poses challenges concerning its optimization as a lead compound. Moreover, we found out a limited enzymatic stereoselective interaction, being the two enantiomers almost equally active against HDAC6. Consequently, since the preparation of enantiopure tools could be challenging, we decided to investigate a new scaffold, easy to synthesize through a one-pot multicomponent strategy[28], designed to exhibit a therapeutic potential against IPF.

In this work, combining synthetic, computational and biological efforts,[18,25,29–32] we developed a new series of histone deacetylase inhibitors **5a-o**, preferentially targeting HDAC6, as potential modulators of the IPF-related fibrosis. The rational design of the new compounds thoroughly relied on the exploitation of the general pharmacophore features of HDACis: *i*) the cap group, the surface recognition moiety, *ii*) the zinc-binding group (ZBG), capable of tightly chelating the Zn^{2+} ion located in the active site, and *iii*) the linker tethering the two portions (**Figure 1**). The spirotetrahydroisoquinoline (STHIQ) was selected as a cap group (**Figure 1**).

For a quick synthesis of the new STHIQ inhibitors **5a**-**o** (**Figure 1** and **Table 1**) we explored the Castagnoli-Cushman three-component reaction (CCR), which ensured a straightforward analoging at the quaternary spiro-carbon center.[33] The enzymatic assay guided the identification of four hit compounds (**5k**, **5l**, **5m** and **5n**) exhibiting an interesting HDAC6 potency profile over a selected panel of isoforms (HDAC1, 8, 10) except for **5n** which was tested against a further panel of six HDAC isoforms (HDAC1,3,5,8,10,11) (**Table 2**). Target engagement was assessed for the best-performing candidates in cell-based assays, by determining the acetylation levels of histone H3 and α-tubulin, the main non-histone substrate of HDAC6.[14] A preliminary evaluation of the physicochemical properties enabled the selection of the best hit **5n** (**Table S1**) which was interrogated for its ability to attenuate the fibrotic process in both HLFs and cultured cells isolated

from BAL fluid of IPF patients. The toxicity profile of **5l** and **5n** was measured in vivo using a zebrafish model while the cardiotoxic potential of **5n** was investigated in functional studies.

Table 1. Inhibitory activity of compounds **5a**-**o** toward *h*HDAC6 (as IC_{50}, nM).

Cpd	Structure	*h*HDAC6 (IC_{50} nM)	Cpd	Structure	*h*HDAC6 (IC_{50} nM)
5a	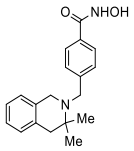	263 ± 17	**5i**	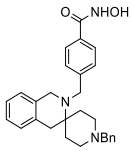	313 ± 22
5b	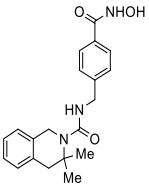	133 ± 18	**5j**	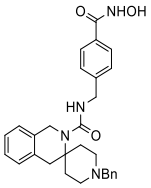	142 ± 11
5c	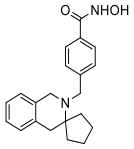	667 ± 41	**5k**	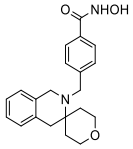	101 ± 7
5d	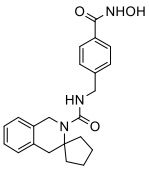	212 ± 14	**5l**	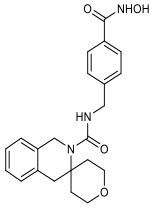	115 ± 8
5e	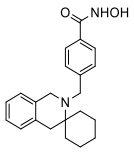	1745 ± 129	**5m**	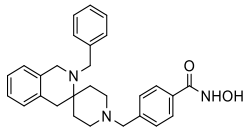	148 ± 10
5f	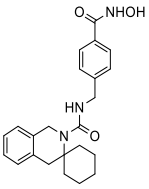	245 ± 17	**5n**	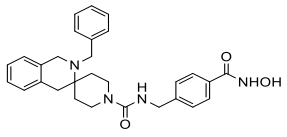	63± 4
5g	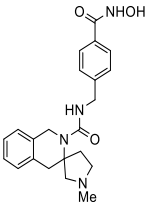	277 ± 17	**5o**	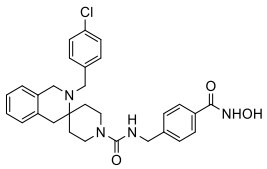	77 ± 5
5h	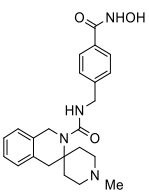	380 ± 21	**2**		40.8 ± 1.51

Each value is the mean of at least three determinations; results are expressed as mean ± standard error of the mean (SEM).

Table 2. Inhibitory activity of selected compounds toward, *h*HDAC1, *h*HDAC10, *h*HDAC8, *h*HDAC3, *h*HDAC5 and *h*HDAC11 (as IC_{50}, nM).

Cpd	IC_{50} (nM)					
	***h*HDAC1**	***h*HDAC8**	***h*HDAC10**	***h*HDAC3**	***h*HDAC5**	***h*HDAC11**
5k	1493 ± 97	>10000 (4%)	9725 ± 632	NT[a]	NT[a]	NT[a]
5l	3912 ± 243	1327 ± 93	7300 ± 458	NT[a]	NT[a]	NT[a]
5m	1242 ± 88	3407 ± 219	9044 ± 671	NT[a]	NT[a]	NT[a]
5n	1472 ± 89	2533 ± 167	5329 ± 368	1451 ± 102	>10000 (23%)	640 ± 41
2	5421 ± 268	2204 ± 198	NT[a]	5871 ± 376	>10000 (14%)	695 ± 41

Each value is the mean of at least three determinations; results are expressed with ± standard error of the mean (SEM); NT[a], not tested.

RESULTS AND DISCUSSION

Chemistry

For the synthesis of STHIQ compounds **5a**-**o** we applied and implemented a flexible and streamlined strategy for the introduction of a spiro system at C3 in the THIQ nucleus (**Figure 1**).

The compounds were prepared following two different chemical paths based on CCR as the key step to construct the spiro-scaffold as tetrahydroisoquinolonic acid (**Figure 1** and **Scheme 1**).[33]

For the first set of derivatives **5a**-**l**, a retrosynthetic analysis has guided the identification of the synthons **6a**-**g** which could be obtained *via* CCR starting from the homophthalic anhydride (**7**), the appropriate cyclic ketones (**8a**-**g**), and ammonium acetate.

The synthesis of the analogues **5m**-**o** required the preparation of the key intermediate **9** by applying the same CCR protocol with the suitable *N*-protected piperidone (**8f** or **11**) as a ketone, and the primary amines **12** or **13** in place of the ammonium acetate (**Figure 1** and **Scheme 1**).

For a rapid analoging, the use of amines in place of ammonium acetate was investigated by us, thus expanding the chemical space achievable by this CCR protocol.

For the synthesis of the intermediates **6a**-**g**, the one-pot CCR was performed by reacting **7**, **8a**-**g**, and ammonium acetate in acetonitrile at 80 °C.

The CCR crude products were used for the decarboxylation step which allowed to remove a stereogenic center, furnishing the tetrahydroisoquinolones **14a**-**g**.

These latter underwent reduction by $LiAlH_4$[34] at high temperature, affording the corresponding STHIQs **15a**-**g**. Under these conditions, the *N*-Boc function of the intermediate **14d** was simultaneously reduced, affording the desired *N*-methyl derivative **15d**.

Scheme 1. Synthesis of the STHIQ derivatives **5a-o**.

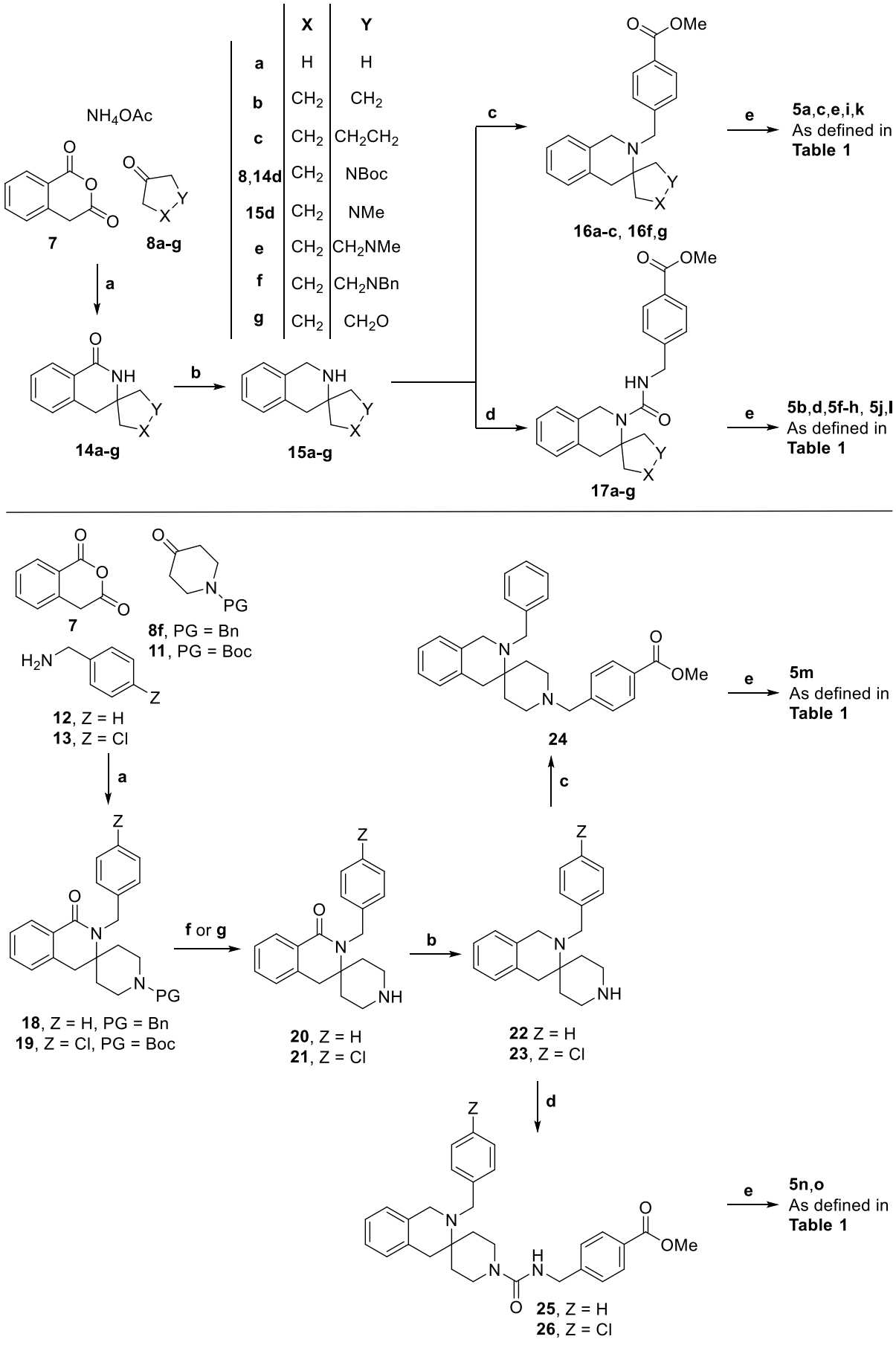

[a]Reagents and conditions: **a)** (*i*) MeCN, 80 °C, 12 h; (*ii*) K_2CO_3, DMSO, 175 °C, 90 min (16-69% yield); **b)** $LiAlH_4$, dry 1,4-dioxane, N_2, from 0 °C to 100 °C, 20 h (59-100% yield); **c)** methyl 4-

(bromomethyl)benzoate, K_2CO_3, dry DMF, N_2, 75 °C, 12 h (46-70% yield); **d)** methyl 4-(isocyanatomethyl)benzoate, dry TEA, dry THF, N_2, 25 °C, 12 h (36-90% yield); **e)** NH_2OH (50 wt.% in H_2O), KOH (4 M in MeOH), MeOH, from 0 °C to 25 °C, 3 h (20-78% yield); **f)** H_2, Pd/C, MeOH, 25 °C, 30 min, for **20** (84% yield); **g)** HCl/MeOH, MeOH, 40 °C, 30 min, for **21** (100% yield).

The STHIQ core of the intermediates **15a**-**g** was appropriately functionalized as tertiary amine or urea in the presence of the suitable linker moiety. Nucleophilic substitution of **15a**-**c**, and **15f**-**g** with methyl 4-(bromomethyl)benzoate in the presence of potassium carbonate gave the corresponding tertiary amines **16a**-**c**, and **16f**,**g**. The intermediates **15a**-**g** were also reacted with methyl 4-(isocyanatomethyl)benzoate, freshly prepared according to the literature procedure,[35] to obtain the ureas **17a**-**g**.[36,37] The methyl ester derivatives **16a**-**c**, **16f**,**g** and **17a**-**g** were treated with the aqueous hydroxylamine solution, and potassium hydroxide to afford the title compounds **5a**-**l**.[38] The synthetic approach developed for the title compounds **5m**-**o** is also described in **Scheme 1**. The application of the above mentioned CCR protocol allowed to obtain the non-isolated intermediates **9** and **10** starting from **7**, **12** or **13**, and the *N*-protected piperidone (**8f** or **11**).[39] The decarboxylation of the CCR product **9** and **10** gave the lactams **18** and **19**, respectively. Compound **18** underwent catalytic hydrogenation for the cleavage of the benzyl group on the spiropiperidine moiety, yielding the derivative **20**, while Boc-deprotection of **19** furnished the intermediate **21**. Both amines were in turn converted into the STHIQs, namely **22** and **23**, after reduction operated by $LiAlH_4$. The intermediate **22** was combined with methyl 4-(bromomethyl)benzoate or methyl 4-(isocyanatomethyl)benzoate to generate the methyl esters **24** and **25**, respectively. These latter were subjected to the transamidation protocol with hydroxylamine under basic condition, providing the title compounds **5m** and **5n**. Analogously, the derivative **23** was combined with the methyl(isocyanatomethyl)benzoate furnishing the urea **26** which was finally converted into the corresponding hydroxamic acid **5o**, after treatment with aqueous NH_2OH, and KOH.

Structure activity relationship analysis, *in vitro* HDAC inhibition and molecular modelling studies

For the first set of compounds (**5a**-**l,** 101<IC_{50}<1745 nM), the STHIQ core was combined, either directly or through a urea motif, to the benzyl linker bearing the ZBG. To expand this initial set of compounds and gain additional structure-activity relationship (SAR) information, we exploited the spiropiperidine template to perform the overturning of the linker moiety from the nitrogen of the THIQ to the nitrogen of the spiro group, and thus obtaining the second set of derivatives **5m**-**o** (63<IC_{50}<148 nM). Docking simulations (see methods for details) showed that the THIQ hit **5a** (IC_{50} = 263 nM) could be easily accommodated into the *h*HDAC6 active site (**Figure 2A**) with the hydroxamic acid group able to chelate the zinc atom, with its basic nitrogen, modelled in its protonated form ($pK_{a,exp}$ = 9.53)[40], able to undertake favorable interactions with Ser568 (Ser531 in *Danio rerio HDAC6*), a residue known to be important for ensuring potency and selectivity versus HDAC6.[41] The docking output presented in **Figure 2A** confirmed that the two synthetic strategies described before, the first based on the installation of a spiro substituent at C3 position of the THIQ (exemplified by **5k,** IC_{50} = 101 nM) and the second on the carbamoylation of the THIQ nitrogen moiety to give ureidic derivatives (exemplified by **5b**, IC_{50} = 133 nM and **5l**, IC_{50} = 115 nM), could lead to better compounds than **5a**. As for the first approach, the installation of a hexahydropyran nucleus at the THIQ position 3 led to compound **5k** (IC_{50} = 101 nM), nearly 3-fold more potent than **5a**, possibly thanks to key polar interactions undertaken with His651, through the interposition of a conserved water molecule (**Figure 2B**), present in several X-ray structures of HDAC6 in complex with hydroxamic acid inhibitors.[41,42] The importance of the polar interaction undertaken by the pyran oxygen with the HDAC6 is supported by the modest activity of the spiro cyclohexane derivative **5e** (IC_{50} = 1745 nM). As for the second approach, the introduction of a carbamoyl spacer in **5a** had a positive effect on the inhibition potency (compound **5b**, IC_{50} = 133 nM), due to an optimal accommodation of the urea group at the HDAC6 active site entrance. The urea was indeed able to form a hydrogen bond (H-bond) with the key residue Ser568 (**Figure 2C**). It is worth mentioning that, for the ureido-based inhibitors reported in **Table 1**, the installation of a spiro ring at C3 of the THIQ scaffold always led to less active compounds than **5b**, with the only exception of the hexahydropyran derivative **5l** (IC_{50} = 115 nM), able to form a H-bond with the backbone NH of Phe680 (**Figure 2D**).

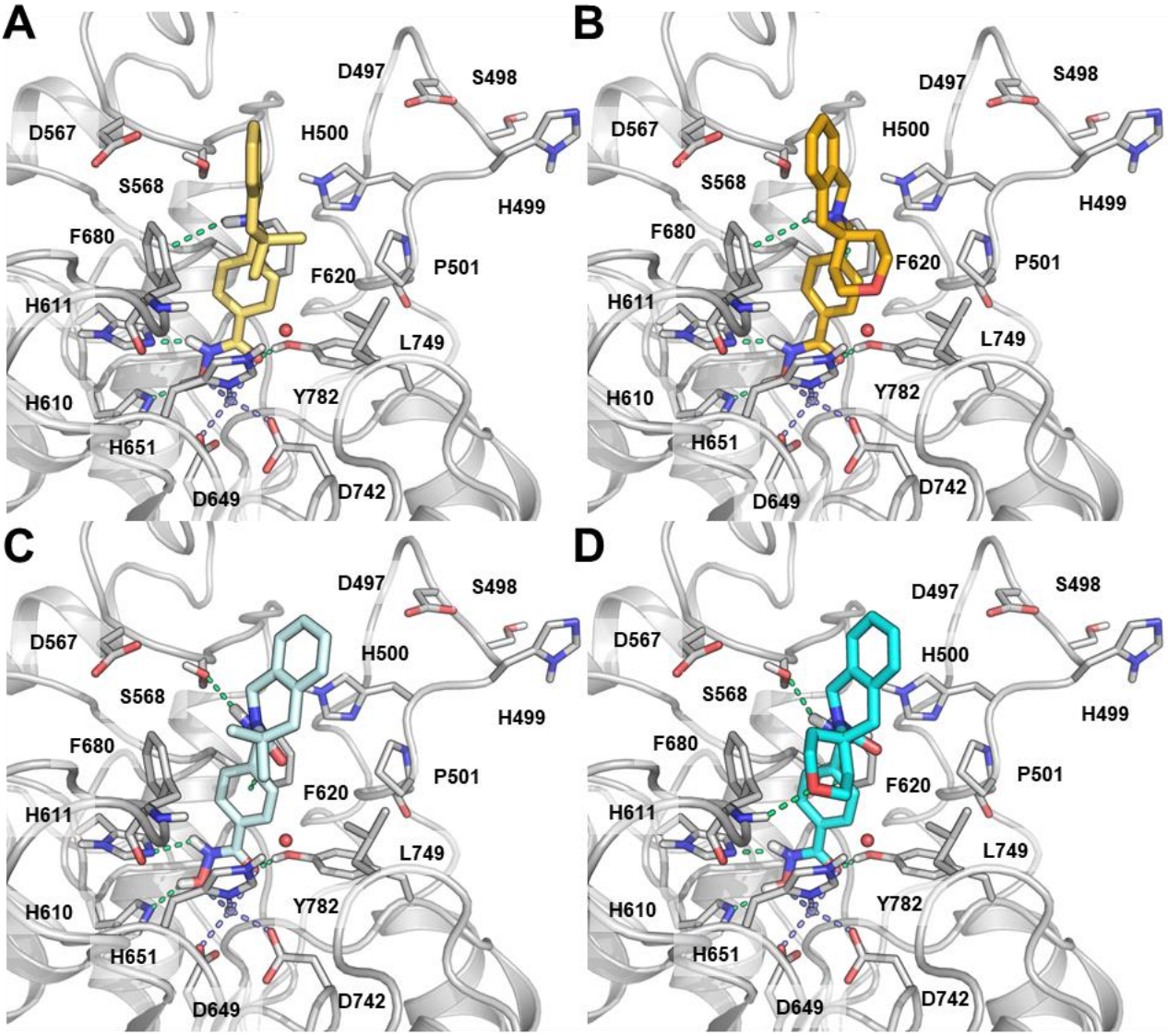

Figure 2. Docking poses of **5a** (panel A, yellow carbon atoms), **5k** (panel B, orange carbon atoms), **5b** (panel C, light cyan carbon atoms) and **5l** (panel D, cyan carbon atoms) within the binding site of hHDAC6 (grey carbon atoms and cartoon). Coordination bonds between the Zn^{2+} ion (violet sphere) and hydroxamic group and protein residues are represented with violet dashed lines, while H-bonds and π-π interactions between the ligands are represented with green dashed lines. A conserved water molecule is also shown as a red sphere (geometries taken from the X-ray structure of *zf*HDAC6 in complex with trichostatin A, PDB code: 5EEK).

We next applied docking simulations to search for a reasonable binding mode for **5n** (IC_{50} = 63 nM), the most potent compound of the whole set of HDAC6 inhibitors, in which the *N*-hydroxybenzamide ZBG was installed on the nitrogen atom of the THIQ scaffold. In the case of **5n**, docking simulations alone failed to produce a reasonable binding mode at the HDAC6 active site. The best poses obtained for this compound (**Figure 3A**) were always characterized by a consistent fitting of ZBG, although the cap group (i.e., a 2-benzyl-1,4-dihydro-2H-spiro[isoquinoline-3,4'-

piperidine]-1'-carboxamide substructure failed to establish productive interactions with HDAC6. We thus used molecular dynamics (MD) simulations (see methods for details) to better sample the conformational space of the docking complexes.[43] Three independent 250 ns-long MD simulations showed that, after the equilibration, the cap group of **5n** experienced a significant rearrangement (compared to the docked poses) which positioned the NH and carbonyl oxygen of the urea group close to Ser568 and to the conserved water molecule bound to His651, respectively. A representative snapshot of one of the MD simulations is reported in **Figure 3B**. Analysis of the MD-trajectories showed that, regardless of the docking pose used as starting point, the ureidic group of compound **5n** was able to form a H-bond with both Ser568 and His651 for a significant fraction of the simulations (**Figure S1**).

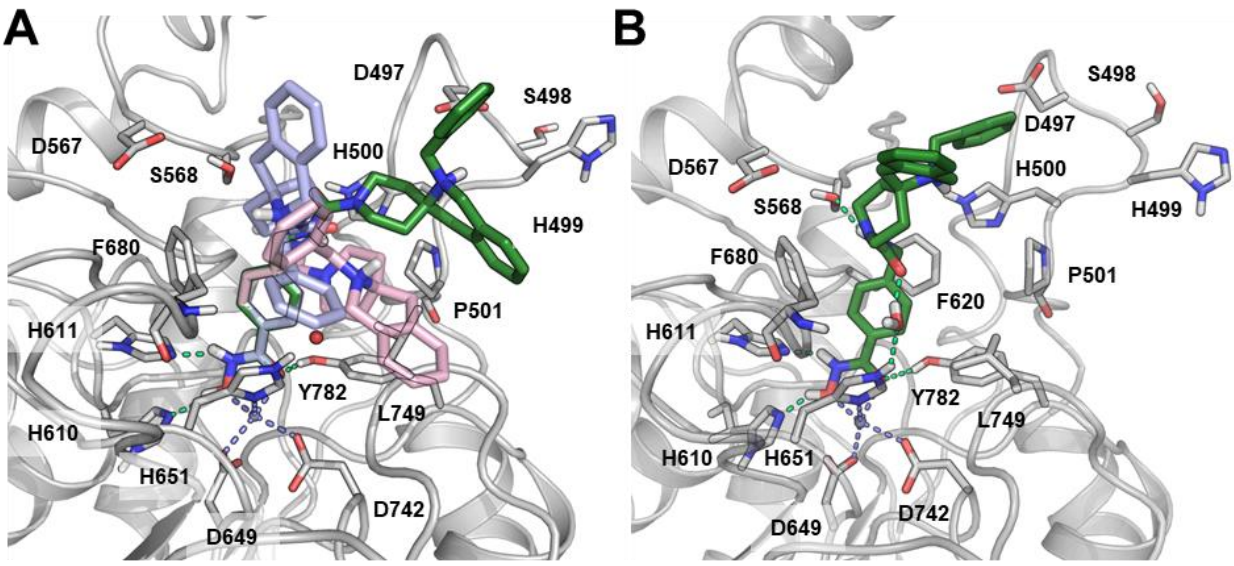

Figure 3. A) Alternative docking poses for compound **5n** (binding pose 1, violet carbon atoms; binding pose 2, pink carbon atoms; binding pose 3, green carbon atoms) within the binding site of hHDAC6 (grey carbon atoms and cartoon). Coordination bonds between the Zn^{2+} ion (violet sphere) and hydroxamic group and protein residues are represented with violet dashed lines, while H-bonds between the hydroxamic group of **5n** and the protein are represented with green dashed lines. A conserved water molecule is also shown as a red sphere. B) Representative snapshot of a 250 ns-long MD simulation performed starting from binding pose 3 (green carbon atoms). During the simulation, a water molecule, superimposed to a conserved X-ray water molecule, mediates a H-bond network between His651 and the ureidic functional group of **5n**.

HDAC6 as a Preferential Target: target engagement by Western Blot analysis

For assessing HDAC6 preferential interaction, the most potent and interesting analogues (**5k**, **5l**, **5m** and **5n**) were engaged in experiments in living cells. The cell-based assays were conducted on

U2OS cells, a cell line stably expressing Class I (i.e. HDAC1) and Class II (i.e. HDAC6) enzymes.[25] We preliminary ascertained that all the tested compounds did not show toxicity in these cells compared to SAHA, Tubastatin A (TUB) and PCI34051 (PCI) from 24 to 72 h of incubation (**Figure S2**). Further, the levels of α-tubulin acetylation (the client protein of HDAC6) and of acetylation of histone H3 (the primary substrate of HDAC1-3) were evaluated after incubation of compounds at 10 μM for 24 h (**Figure 4**). Analogues **5k**, **5l** and **5n** efficiently inhibited HDAC6, inducing marked acetylation of α-tubulin, also compared to TUB. At the same dose, histone H3 acetylation was unchanged, hinting at the preferential interaction of this set of compounds toward the HDAC6 enzyme, with respect to class I HDACs (**Figure 4**).

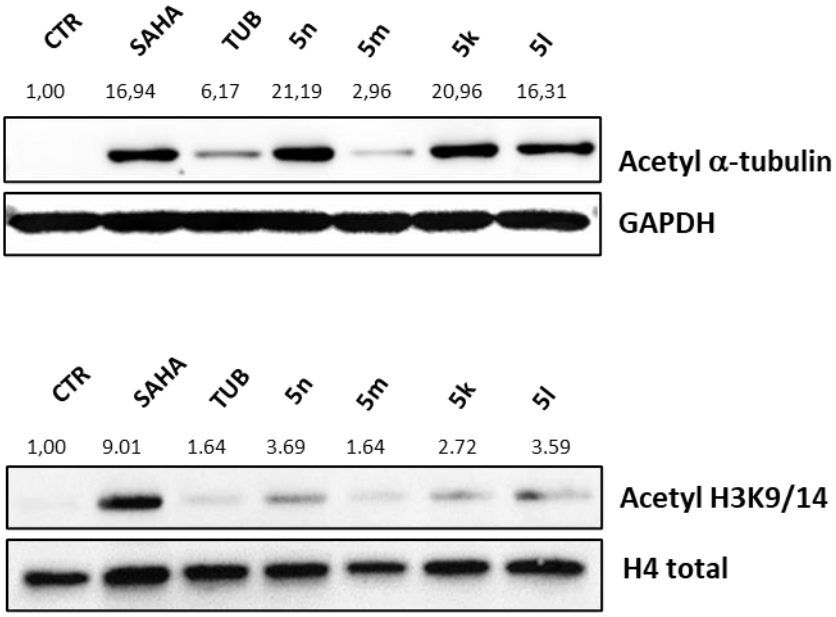

Figure 4. Western Blot analysis of acetylated α-tubulin expression on total protein extract and evaluation of H3 total acetylated expression on histone extract. Semi-quantitative analysis of western blot was performed by using ImageJ software (version 1.44).

Preliminary studies to assess solubility, chemical stabilities and LogP

To establish the potentiality of the novel HDACis as pharmacological tools, we assessed the drug-likeliness of the best-performing compounds, namely **5k**-**n**, by experimentally determining their solubilities and chemical stabilities (**Table S1**). These parameters were measured at pH = 3 and pH = 7.4 by means of HPLC, as previously reported.[44] From this preliminary study, the selected compounds displayed excellent solubility at pH = 3 in the same range values (from 250 to 279 μM).

By contrast, considerable differences in solubility at simulated physiological conditions were observed between the two pairs of derivatives belonging to the two subsets of STHIQ. More in detail, compounds **5k**,**l** exhibited a more favourable solubility at pH = 7.4 with respect to the derivatives **5m**,**n** although maintaining a satisfactory profile. Gratifyingly, all the tested compounds proved to be stable at both pH conditions, with equal or more than 85% of the remaining compound unaffected after 24 h of exposure. LogP was also experimentally determined for compounds **5k,l**-**n** as previously described,[38] and the data are shown in **Table S1**.

In vivo toxicity evaluation of 5l and 5n in zebrafish larvae

To assess the safety of compounds **5l** and **5n** (representative of both subsets of analogues, **Figure 1**), we exposed zebrafish larvae at 3.5 days post-fertilization to progressively higher concentrations of the compounds (25-100 μM). Regarding dose selection, it is common to observe differences in effective doses between zebrafish and in vitro systems. Higher doses are typically required in zebrafish models compared to in vitro models to achieve significant biological effects. This discrepancy is primarily due to variations in drug absorption, distribution, metabolism, and excretion between whole organisms and isolated cells. The dose range is comparable to what already used for other HDAC6 inhibitors in our previous studies.[30,37] In the case of **5n**, one day after exposure, there were no noticeable morphological changes in the zebrafish larvae's body axis (**Figure 5A**-**D**). Additionally, we measured body length and the sizes of the pericardial, yolk, and eye areas as markers for treatment tolerability, and found no significant morphological differences (**Figure 5E**-**H**). Similarly, when examining body morphology (**Figure 5I**-**P**) in zebrafish larvae treated with increasing concentrations of compound **5l**, no significant differences were observed. Together, these results suggest that compounds **5n** and **5l** did not cause appreciable toxic effects in an in vivo system.

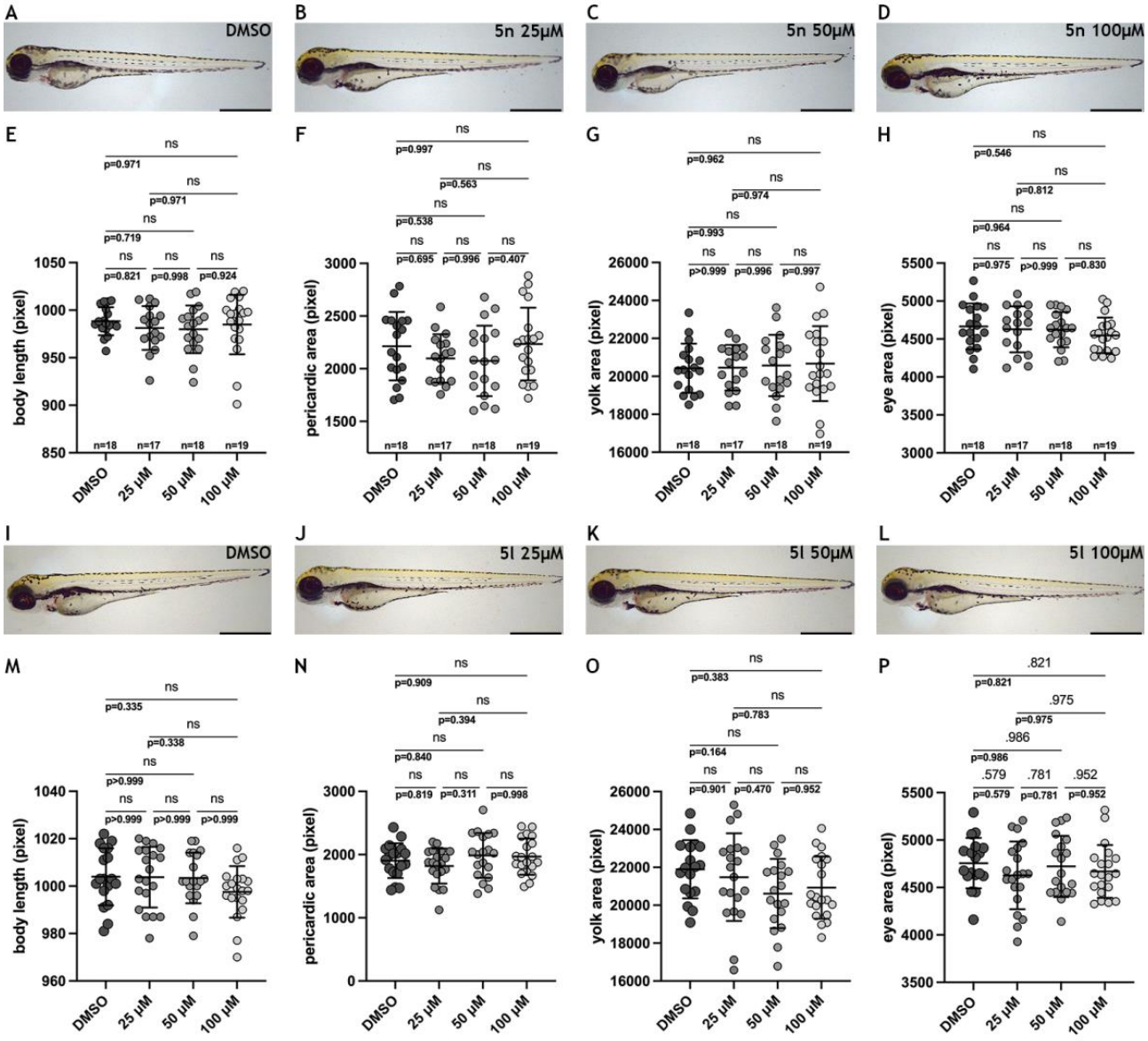

Figure 5. Safety evaluation of compounds 5n and 5l in the in vivo zebrafish model system. **A-D**) Representative images of 3.5 dpf zebrafish larvae treated with **A**) DMSO (n=18) or 5n at the concentration of **B**) 25 µM (n=17), **C**) 50 µM (n=18) and **D**) 100 µM (n=19). n stands for the number of larvae analyzed. Scale bar indicates 300 µm. (**E**-**H**) Histograms representing the quantification analyses of **E**) body length and of **F**) pericardiac, **G**) yolk and **H**) eye areas. Each dot represents the pixel value of a single embryo. Data are presented ad mean±SD. One-Way Anova, Tukey's post-hoc. ns not significant. (**I-L**) Images of 3.5 dpf zebrafish larvae treated with **I**) DMSO (n=18) or **5l** at the concentration of **J**) 25 µM (n=20), **K**) 50 µM (n=19) and **L**) 100 µM (n=20). n stands for the number of larvae analyzed. Scale bar indicates 300 µm. (**M**-**P**) Histograms representing the quantification analyses of **M**) body length and of **N**) pericardiac, **O**) yolk and **P**) eye areas. Each dot represents the pixel value of a single embryo. Data are presented as mean±SD. One-Way Anova, Tukey's post-hoc. ns not significant.

Toxicity evaluation of 5n on Langendorff perfused rat heart

To evaluate the cardiotoxic potential of compound **5n**, its effect on cardiac mechanical function and electrocardiogram (ECG) in Langendorff-isolated rat hearts was assessed, as previously

described.[45–47] Under control conditions, LVP and CPP values of 69,3 ± 5,5 and 64,7 ± 14,2 mmHg (n = 5) were obtained (**Figure 6**). Up to the highest concentration tested (30 μM), compound **5n** did not affect either LVP or CPP (**Figure 6**), but, in a concentration-dependent manner, significantly reduced HR, prolonging the RR interval (**Table S2**). However, PQ, QRS, and QTc values **5n** did not change over the drug concentration range tested (**Table S2**). The present findings highlight that at the maximum concentration tested, **5n** exhibited negative chronotropic activity and prolonged the cardiac cycle length.

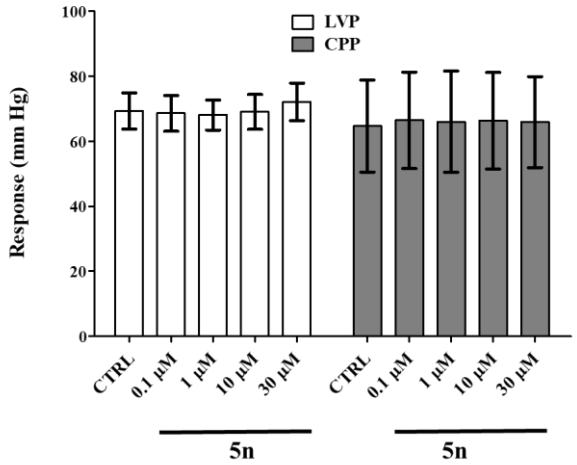

Figure 6. Effects of **5n** on LVP and CPP in Langendorff-perfused rat hearts. Concentration-effect relationship of **5n** on LVP and CPP. On the ordinate scale, the response is reported as mmHg. Each value represents mean±s.e.m. (n=5).

Evaluation of the antifibrotic effects of compound 5n on human ex vivo IPF models

The efficacy of compound **5n** as a new potential anti-IPF agent was investigated in two ex vivo models, namely the cultured bronchoalveolar-lavage-derived fibroblast cells (B-LSDM7) derived from BAL fluid of a cohort of IPF patients (**Figure 7A-D** and **Figure 7I-L**) and the primary HLF cell line (**Figure 7E-H** and **Figure 7M-P**). Specifically, the antifibrotic properties of **5n** were compared to those of **2**, taken as a reference compound, by evaluating their ability to modulate the expression of the typical biomarkers of the TGF-β1-dependent fibrosis (collagen I, fibronectin, vimentin and α-SMA) and to detect the viability after compounds administration (**Figure S4**).

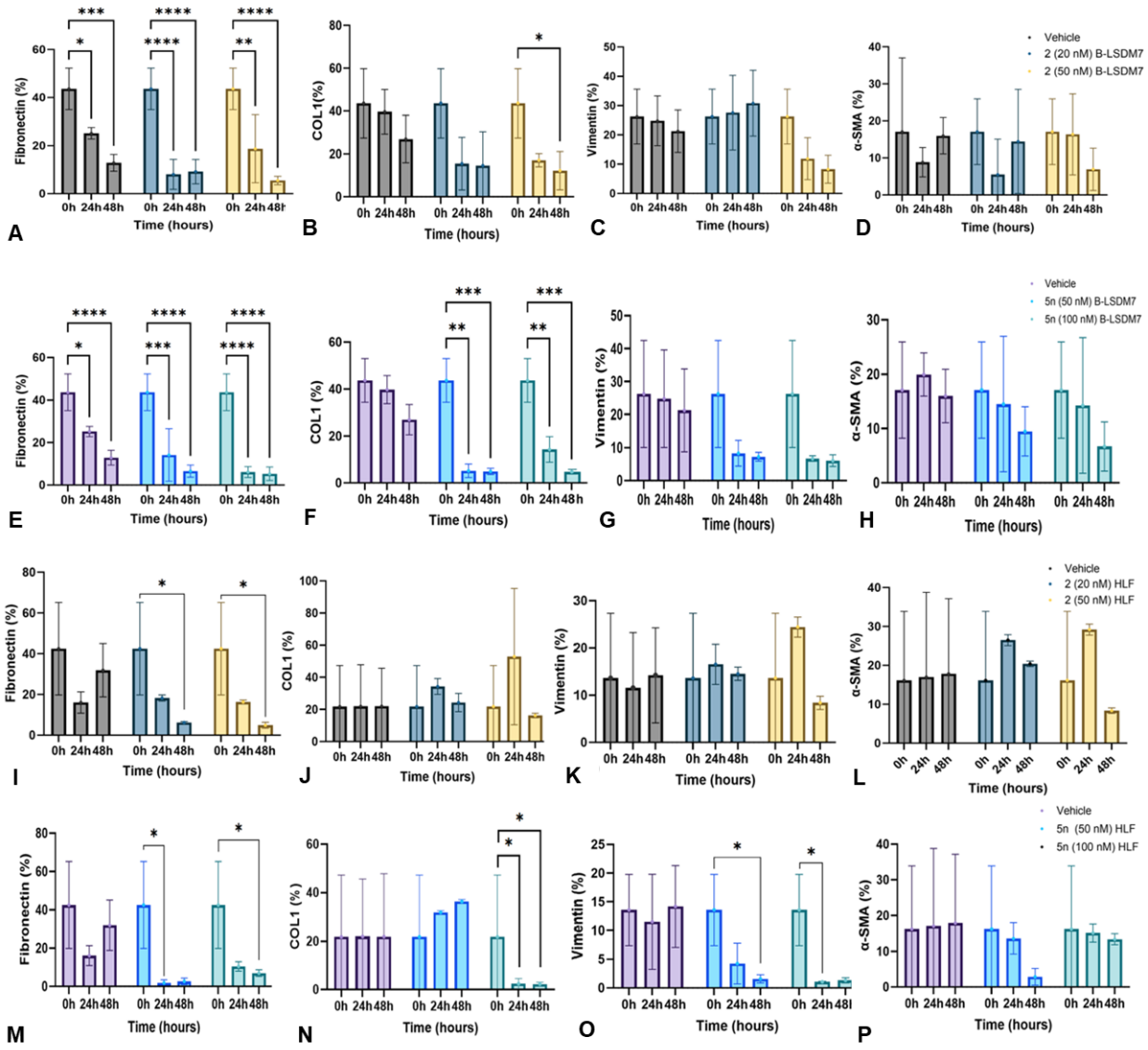

Figure 7. A-P) Fibronectin, vimentin, COL1 and α-SMA expression levels in BLSDM-7 and HLF cells (n = 3) at 0, 24 and 48 h. Data are reported as mean *SE. ****p < 0.0001, ***p < 0.001 **p < 0.01, *p < 0.05.

The results showed that compound **2** downregulated fibronectin after 24 and 48 h of treatments at 20 and 50 nM in B-LSDM7 cells (**Figure 7A**). Further, the treatment with **2** at 50 nM resulted in a decreased expression of collagen type 1 (COL1) after 48 h of incubation (**Figure 7B**), while no significant differences emerged for vimentin and α-SMA expression (**Figure 7C-D**). Similarly, the administration of **5n** in B-LSDM7 cells negatively modulated the expression of fibronectin and COL1 after 24 and 48 h (**Figure 7E,F**), while leading to a moderate downregulation of vimentin and α-SMA without reaching the significance (**Figure 7G,H**). Treatments of HLF cell line with either **2** or **5n** reduced the expression of fibronectin after 24 and 48 h (**Figure 7I-M**). Moreover, compound **5n**

negatively affected the expression of COL1 (**Figure 7N**) and effectively decreased vimentin expression after 48 h of treatment at 50 nM and after 24 h of treatment at 100 nM in primary HLF cell line (**Figure 7O**). No effects were detected for the expression of α-SMA in both cell lines (**Figure 7L,P**). As reported in literature, it is very difficult to find homogeneous information about the modulation of α-SMA in fibrotic conditions. Some studies reported that HDAC6is could reduce the expression of α-SMA with no appreciable statistical significance and at high doses if compared to the therapeutic ones.[25,27] Other works reported no modulation of α-SMA, indicating that the expression levels were not reduced under inhibitor pressure.[48,49]

Accordingly, some studies revealed also that the importance of α-SMA in tissue fibrogenesis varies among different tissues, thus limiting its eligibility as a functional marker of fibrosis.[50,51]

The two compounds **2** and **5n** were also evaluated for their potential toxicity, with no appreciable toxic effect at the doses tested in the two ex vivo models (**Figure S4)**.

In summary these results highlight the better profile of **5n** compared to **2** as, by reducing the expression of vimentin, the compound could limit the invasiveness of lung fibroblasts.[52]

5n modulates HDAC6 activity in a human ex vivo IPF model

HDAC6 activity was measured after the treatments with compounds **2** and **5n** in B-LSDM7 and HLF cells (**Figure 8**). HDAC6 activity resulted decreased in B-LSDM7 cells when treated with compound **2** at 50 nM (p=0,03), while **5n** was able to reduce HDAC6 activity in B-LSDM7 cells when treated at 50 and 100 nM, when compared to vehicle (p=0,04 for each concentration). In HLF cells the reduction of HDAC6 activity was visible at the same doses but with no statistical significance. The data reported in this study highlighted the intriguing role of HDAC6is in reversing IPF phenotype. This topic is highly challenging considering also that the only available drugs, pirfenidone and nintedanib, do not reverse or cure IPF. There is a pressing need for new pharmacological interventions that can slow down or stop disease progression and ultimately cure this condition. Different drugs and combination of drugs have been proposed over the years, but none of them reached clinical trials due to side effects.[53]

In this context, the investigation at the molecular level in the fibrotic process is fundamental to decipher targeted therapies that could potentially stop the progression of the disease. Future directions include personalized medicine approaches, artificial intelligence integration, growth in genetic insights, and novel drug targets,[54] like HDAC enzymes, particularly HDAC6, which could provide a new interesting therapeutic option for IPF treatment.[55]

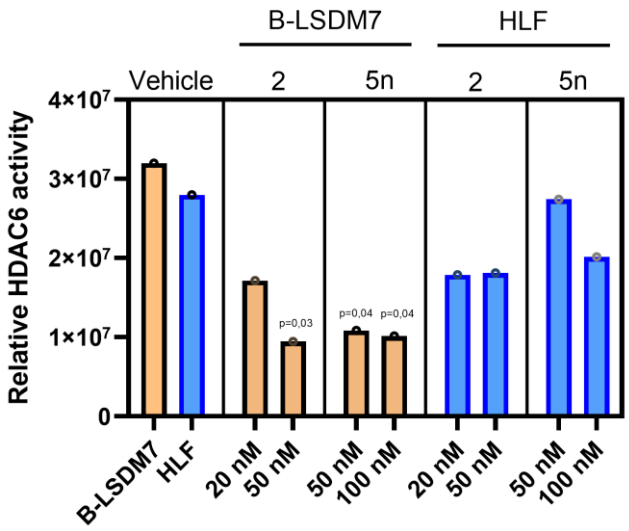

Figure 8. HDAC6 activity assay measured in B-LSDM7 and HLF cells. Data represent measurements from 2 independent replicates.

CONCLUSION

We report herein the synthesis and ex vivo evaluation of new STHIQ-based histone deacetylase inhibitors obtained by applying the facile and versatile one-pot Castagnoli-Cushmann reaction protocol for the assembly of the spiroscaffold. This multicomponent protocol guaranteed rapid synthesis and analoging. The compounds were analyzed for their inhibitory activity against HDAC6 showing IC_{50} values ranging from 63 to 1745 nM. The derivative **5n**, the most potent compound of the series, showed HDAC6 preferential inhibition compared to HDAC1, HDAC3, HDAC5, HDAC8, HDAC10 and HDAC11.

When docked into human HDAC6 active site, the 2-benzyl-1,4-dihydro-2H-spiro[isoquinoline-3,4'-piperidine]-1'-carboxamide moiety experienced a significant rearrangement to position its ureidic hydrogen close to Ser568, and the carbonyl oxygen close to a conserved water molecule H-bonding His651. **5n** did not show toxicity in rat-perfused heart and in vivo on zebrafish larvae. **5n**

was able to increase levels of acetylated α-tubulin compared to histone H3 at 10 μM in living cells, demonstrating the target engagement. In ex vivo models of IPF, **5n** was able to negatively modulate the expression of fibrotic markers fibronectin and Col1 in cells derived from bronchoalveolar lavage of IPF patients (B-LSDM7). In HLF human IPF model, **5n** reduced the expression of fibronectin and negatively affected the expression of vimentin, this latter being associated with the invasiveness of the fibrotic process. In conclusion, a new pharmacological tool was identified as a potent anti-fibrotic agent modulating HDAC6 activity in two human IPF ex-vivo models.

METHODS

Methods are reported in the Supporting Information[46,56,57]

Supporting Information

Chemistry Section: synthesis and characterization of compounds **5a**-**o**. Molecular modelling section: docking and molecular dynamics simulations protocols. Biological Section: cell viability, target engagement, cell viability, in vivo studies

Acknowledgements

Giuseppe Campiani and Stefania Butini thank Next Generation EU – National Recovery and Resilience Plan (NRRP) – Mission 4 Component 2 Investment 1.4 – Italian Ministry of University and Research (MUR) Project Code ECS_00000017 MUR Directoral Decree n.1055 , 23 June 2022, CUP B83C22003930001, "Tuscany Health Ecosystem – THE" - Spokes 7-8. Giuseppe Campiani, Elena Bargagli and Stefania Butini thank Regione Toscana IT for the grant Bando Ricerca Salute 2018-Regione Toscana – HIDE-IPF, "Epigenetic and proteomic approaches towards innovative targeted therapies for IPF". Anna Pistocchi, Alex Pezzotta, Sabrina Carbone and Giuseppe Campiani are supported by the AIRC-Investigator Grant- IG 2023, code 29187. Sabrina Carbone was supported by the PhD program in Experimental Medicine of the University of Milan, Milan, Italy. Rosaria Benedetti thank PNRR-MAD-2022–12376723; PNRR-CN3, National Centre

for Gene Therapy and Drugs Based on RNA Technology, cod:CN000000041. Lucia Altucci thank EPI- MET Fondo Crescita Sostenibile—Accordi per l'Innovazione di cui al D.M. 31.12.2021 e D.D. 18.03.2022 Progetto posizione n. 34; n. progetto F/310034/03/X56. PRIN P2022F3YRF. Chiara Papulino thank project n. PNC0000003—AdvaNced Technologies for Human-centrEd Medicine (project acronym: ANTHEM). This research benefits from the High Performance Computing facility of the University of Parma, Italy (HPC.unipr.it). This work has been carried out in the frame of the ALIFAR project, funded by the Italian Ministry of University through the program 'Dipartimenti di Eccellenza 2023-2027'.

Author Information

Anna Fontana 0000-0002-5091-8202 a.fontana5@student.unisi.it

Laura Bergantini 0000-0002-1118-3223 laura.bergantini@unisi.it

Gabriele Carullo 0000-0002-1619-3295 gabriele.carullo@unisi.it

Laura Scalvini 0000-0003-3610-527X laura.scalvini@unipr.it

Miriana d'Alessandro 0000-0002-2368-5722 miriana.dalessandro@unisi.it

Chiara Papulino 0000-0003-4743-3017 chiara.papulino@unicampania.it

Paolo Cameli 0000-0001-8639-2882 paolo.cameli@unisi.it

Sara Gangi 0000-0003-1834-535X sara.gangi@student.unisi.it

Fabrizio Vincenzi 0000-0002-5027-1699 fabrizio.vincenzi@unife.it

Katia Varani 0000-0003-4562-1348 vrk@unife.it

Chiara Contri 0000-0003-3936-5923 chiara.contri@unife.it

Silvia Pasquini 0000-0001-9442-1428 psqslv@unife.it

Anna Pistocchi 0000-0001-9467-2542 anna.pistocchi@unimi.it

Alex Pezzotta 0000-0003-1788-5880 alex.pezzotta@unimi.it

Sabrina Carbone 0009-0000-4119-8971 sabrina.carbone@unimi.it

Simona Saponara 0000-0002-3831-8669 simona.saponara@unisi.it

Sandra Gemma 0000-0002-8313-2417 gemma@unisi.it

Lucia Altucci 0000-0002-7312-5387 lucia.altucci@unicampania.it

Rosaria Benedetti 0000-0001-5517-5519 rosaria.benedetti@unicampania.it

Alessio Lodola 0000-0002-8675-1002 alessio.lodola@unipr.it

Marco Mor 0000-0003-0199-1849 marco.mor@unipr.it

Elena Bargagli 0000-0002-8351-3703 elena.bargagli@unisi.it

Stefania Butini 0000-0002-8471-0880 butini3@unisi.it

Giuseppe Campiani 0000-0001-5295-9529 campiani@unisi.it

*Corresponding authors

Sandra Gemma − Department of Biotechnology, Chemistry and Pharmacy, University of Siena, Siena 53100, Italy; orcid.org/0000-0002-8313-2417; Email: gemma@unisi.it

Giuseppe Campiani − Department of Biotechnology, Chemistry and Pharmacy, University of Siena, Siena 53100, orcid.org/0000-0001-5295-9529; Email: campiani@unisi.it

REFERENCES

(1) Moss, B. J.; Ryter, S. W.; Rosas, I. O. Pathogenic Mechanisms Underlying Idiopathic Pulmonary Fibrosis. *Annu Rev Pathol* **2022**, *17*, 515–546. https://doi.org/10.1146/ANNUREV-PATHOL-042320-030240.

(2) Brindisi, M.; Saraswati, A. P.; Brogi, S.; Gemma, S.; Butini, S.; Campiani, G. Old but Gold: Tracking the New Guise of Histone Deacetylase 6 (HDAC6) Enzyme as a Biomarker and Therapeutic Target in Rare Diseases. *J Med Chem* **2020**, *63* (1), 23–39. https://doi.org/10.1021/acs.jmedchem.9b00924.

(3) Fontana, A.; Cursaro, I.; Carullo, G.; Gemma, S.; Butini, S.; Campiani, G. A Therapeutic Perspective of HDAC8 in Different Diseases: An Overview of Selective Inhibitors. *International Journal of Molecular Sciences 2022, Vol. 23, Page 10014* **2022**, *23* (17), 10014. https://doi.org/10.3390/IJMS231710014.

(4) Selman, M.; Pardo, A. The Leading Role of Epithelial Cells in the Pathogenesis of Idiopathic Pulmonary Fibrosis. *Cell Signal* **2020**, *66*, 109482. https://doi.org/10.1016/J.CELLSIG.2019.109482.

(5) Du Bois, R. M. Strategies for Treating Idiopathic Pulmonary Fibrosis. *Nat Rev Drug Discov* **2010**, *9* (2), 129–140. https://doi.org/10.1038/NRD2958.

(6) Puscas, M.; Martineau, G.; Bhella, G.; Bonnen, P. E.; Carr, P.; Lim, R.; Mitchell, J.; Osmond, M.; Urquieta, E.; Flamenbaum, J.; Iaria, G.; Joly, Y.; Richer, É.; Saary, J.; Saint-Jacques, D.; Buckley, N.; Low-Decarie, E. Rare Diseases and Space Health: Optimizing Synergies from Scientific Questions to Care. *NPJ Microgravity* **2022**, *8* (1), 58–58. https://doi.org/10.1038/S41526-022-00224-5.

(7) Bonella, F.; Spagnolo, P.; Ryerson, C. Current and Future Treatment Landscape for Idiopathic Pulmonary Fibrosis. *Drugs* **2023**, *83* (17), 1581–1593. https://doi.org/10.1007/S40265-023-01950-0.

(8) Bargagli, E.; Piccioli, C.; Rosi, E.; Torricelli, E.; Turi, L.; Piccioli, E.; Pistolesi, M.; Ferrari, K.; Voltolini, L. Pirfenidone and Nintedanib in Idiopathic Pulmonary Fibrosis: Real-Life Experience in an Italian Referral Centre. *Pulmonology* **2019**, *25* (3), 149–153. https://doi.org/10.1016/J.PULMOE.2018.06.003.

(9) Yanagihara, T.; Chong, S. G.; Vierhout, M.; Hirota, J. A.; Ask, K.; Kolb, M. Current Models of Pulmonary Fibrosis for Future Drug Discovery Efforts. *Expert Opin Drug Discov* **2020**, *15* (8), 931–941. https://doi.org/10.1080/17460441.2020.1755252.

(10) Landi, C.; Bargagli, E.; Bianchi, L.; Gagliardi, A.; Carleo, A.; Bennett, D.; Perari, M. G.; Armini, A.; Prasse, A.; Rottoli, P.; Bini, L. Towards a Functional Proteomics Approach to the Comprehension of Idiopathic Pulmonary Fibrosis, Sarcoidosis, Systemic Sclerosis and Pulmonary Langerhans Cell Histiocytosis. *J Proteomics* **2013**, *83*, 60–75. https://doi.org/10.1016/J.JPROT.2013.03.006.

(11) Prasse, A.; Carleo, A.; Jaeger, B.; Schupp, J.; Rottoli, P.; Wuyts, W.; Kaminski, N. BAL Cell Transcriptome Predicts Survival in IPF and Can Be Used to Gauge and Model Treatment Effects Interfering with the TGF-Beta Pathway. *European Respiratory Journal* **2018**, *52* (suppl 62), OA5359. https://doi.org/10.1183/13993003.congress-2018.OA5359.

(12) Bergantini, L.; D'alessandro, M.; Gangi, S.; Cavallaro, D.; Campiani, G.; Butini, S.; Landi, C.; Bini, L.; Cameli, P.; Bargagli, E. Bronchoalveolar-Lavage-Derived Fibroblast Cell Line (B-

LSDM7) as a New Protocol for Investigating the Mechanisms of Idiopathic Pulmonary Fibrosis. *Cells* **2022**, *11* (9). https://doi.org/10.3390/CELLS11091441.

(13) Korfei, M.; Mahavadi, P.; Guenther, A. Targeting Histone Deacetylases in Idiopathic Pulmonary Fibrosis: A Future Therapeutic Option. *Cells* **2022**, *11* (10). https://doi.org/10.3390/CELLS11101626.

(14) Ho, T. C. S.; Chan, A. H. Y.; Ganesan, A. Thirty Years of HDAC Inhibitors: 2020 Insight and Hindsight. *J Med Chem* **2020**, *63* (21), 12460–12484. https://doi.org/10.1021/acs.jmedchem.0c00830.

(15) Pulya, S.; Amin, S. A.; Adhikari, N.; Biswas, S.; Jha, T.; Ghosh, B. HDAC6 as Privileged Target in Drug Discovery: A Perspective. *Pharmacol Res* **2021**, *163*. https://doi.org/10.1016/J.PHRS.2020.105274.

(16) Olaoye, O. O.; Watson, P. R.; Nawar, N.; Geletu, M.; Sedighi, A.; Bukhari, S.; Raouf, Y. S.; Manaswiyoungkul, P.; Erdogan, F.; Abdeldayem, A.; Cabral, A. D.; Hassan, M. M.; Toutah, K.; Shouksmith, A. E.; Gawel, J. M.; Israelian, J.; Radu, T. B.; Kachhiyapatel, N.; De Araujo, E. D.; Christianson, D. W.; Gunning, P. T. Unique Molecular Interaction with the Histone Deacetylase 6 Catalytic Tunnel: Crystallographic and Biological Characterization of a Model Chemotype. *J Med Chem* **2021**, *64* (5), 2691–2704. https://doi.org/10.1021/ACS.JMEDCHEM.0C01922.

(17) Miyake, Y.; Keusch, J. J.; Wang, L.; Saito, M.; Hess, D.; Wang, X.; Melancon, B. J.; Helquist, P.; Gut, H.; Matthias, P. Structural Insights into HDAC6 Tubulin Deacetylation and Its Selective Inhibition. *Nat Chem Biol* **2016**, *12* (9), 748–754. https://doi.org/10.1038/NCHEMBIO.2140.

(18) Brindisi, M.; Senger, J.; Cavella, C.; Grillo, A.; Chemi, G.; Gemma, S.; Cucinella, D. M.; Lamponi, S.; Sarno, F.; Iside, C.; Nebbioso, A.; Novellino, E.; Shaik, T. B.; Romier, C.; Herp, D.; Jung, M.; Butini, S.; Campiani, G.; Altucci, L.; Brogi, S. Novel Spiroindoline HDAC Inhibitors: Synthesis, Molecular Modelling and Biological Studies. *Eur J Med Chem* **2018**, *157*, 127–138. https://doi.org/10.1016/J.EJMECH.2018.07.069.

(19) Gerokonstantis, D. T.; Mantzourani, C.; Gkikas, D.; Wu, K. C.; Hoang, H. N.; Triandafillidi, I.; Barbayianni, I.; Kanellopoulou, P.; Kokotos, A. C.; Moutevelis-Minakakis, P.; Aidinis, V.; Politis, P. K.; Fairlie, D. P.; Kokotos, G. N-(2-Aminophenyl)-Benzamide Inhibitors of Class I HDAC Enzymes with Antiproliferative and Antifibrotic Activity. *J Med Chem* **2023**, *66* (20), 14357–14376. https://doi.org/10.1021/ACS.JMEDCHEM.3C01422/SUPPL_FILE/JM3C01422_SI_005.PDB.

(20) Yu, H.; Liu, S.; Wang, S.; Gu, X. A Narrative Review of the Role of HDAC6 in Idiopathic Pulmonary Fibrosis. *J Thorac Dis* **2024**, *16* (1), 688–695. https://doi.org/10.21037/JTD-23-1183/COIF.

(21) Roche, J.; Bertrand, P. Inside HDACs with More Selective HDAC Inhibitors. *Eur J Med Chem* **2016**, *121*, 451–483. https://doi.org/10.1016/J.EJMECH.2016.05.047.

(22) Melesina, J.; Simoben, C. V.; Praetorius, L.; Bülbül, E. F.; Robaa, D.; Sippl, W. Strategies To Design Selective Histone Deacetylase Inhibitors. *ChemMedChem* **2021**, *16* (9), 1336–1359. https://doi.org/10.1002/CMDC.202000934.

(23) Asfaha, Y.; Schrenk, C.; Alves Avelar, L. A.; Hamacher, A.; Pflieger, M.; Kassack, M. U.; Kurz, T. Recent Advances in Class IIa Histone Deacetylases Research. *Bioorg Med Chem* **2019**, *27* (22). https://doi.org/10.1016/J.BMC.2019.115087.

(24) Shen, S.; Picci, C.; Ustinova, K.; Benoy, V.; Kutil, Z.; Zhang, G.; Tavares, M. T.; Pavlíček, J.; Zimprich, C. A.; Robers, M. B.; Van Den Bosch, L.; Bařinka, C.; Langley, B.; Kozikowski, A. P. Tetrahydroquinoline-Capped Histone Deacetylase 6 Inhibitor SW-101 Ameliorates Pathological Phenotypes in a Charcot-Marie-Tooth Type 2A Mouse Model. *J Med Chem* **2021**, *64* (8), 4810–4840. https://doi.org/10.1021/ACS.JMEDCHEM.0C02210.

(25) Campiani, G.; Cavella, C.; Osko, J.; Brindisi, M.; Relitti, N.; Brogi, S.; Saraswati, A. P.; Federico, S.; Chemi, G.; Maramai, S.; Carullo, G.; Jaeger, B.; Carleo, A.; Benedetti, R.; Sarno, F.; Lamponi, S.; Rottoli, P.; Bargagli, E.; Bertucci, C.; Tedesco, D.; Herp, D.; Senger, J.; Ruberti, G.; Saccoccia, F.; Saponara, S.; Gorelli, B.; Valoti, M.; Kennedy, B.; Sundaramurthi, H.; Butini, S.; Jung, M.; Roach, K.; Altucci, L.; Bradding, P.; Christianson, D.; Gemma, S.; Prasse, A. Harnessing the Role of HDAC6 in Idiopathic Pulmonary Fibrosis: Design, Synthesis, Structural Analysis, and Biological Evaluation of Potent Inhibitors. *J Med Chem 64* (14), 9960–9988. https://doi.org/10.1021/acs.jmedchem.1c00184.

(26) Li, Y.; Yang, H.; Zhao, X.; Zhao, X.; Quan, J.; Wang, L.; Ma, E.; Ma, C. Discovery of Novel Pyrrolo[2,1-c][1,4]Benzodiazepine-3,11-Dione (PBD) Derivatives as Selective HDAC6 Inhibitors for the Efficient Treatment of Idiopathic Pulmonary Fibrosis (IPF) in Vitro and in Vivo. *Eur J Med Chem* **2024**, *275*, 116608. https://doi.org/10.1016/J.EJMECH.2024.116608.

(27) Yu, W. C.; Yeh, T. Y.; Ye, C. H.; Chong, P. C. T.; Ho, Y. H.; So, D. K.; Yap, K. Y.; Peng, G. R.; Shao, C. H.; Jagtap, A. D.; Chern, J. W.; Lin, C. S.; Lin, S. P.; Lin, S. L.; Yu, S. H.; Yu, C. W. Discovery of HDAC6, HDAC8, and 6/8 Inhibitors and Development of Cell-Based Drug Screening Models for the Treatment of TGF-β-Induced Idiopathic Pulmonary Fibrosis. *J Med Chem* **2023**, *66* (15), 10528–10557. https://doi.org/10.1021/ACS.JMEDCHEM.3C00644/SUPPL_FILE/JM3C00644_SI_003.ZIP.

(28) McVicker, R. U.; O'Boyle, N. M. Chirality of New Drug Approvals (2013-2022): Trends and Perspectives. *J Med Chem* **2024**, *67* (4), 2305–2320. https://doi.org/10.1021/ACS.JMEDCHEM.3C02239/SUPPL_FILE/JM3C02239_SI_002.XLSX.

(29) Saraswati, A. P.; Relitti, N.; Brindisi, M.; Osko, J. D.; Chemi, G.; Federico, S.; Grillo, A.; Brogi, S.; McCabe, N. H.; Turkington, R. C.; Ibrahim, O.; O'Sullivan, J.; Lamponi, S.; Ghanim, M.; Kelly, V. P.; Zisterer, D.; Amet, R.; Hannon Barroeta, P.; Vanni, F.; Ulivieri, C.; Herp, D.; Sarno, F.; Di Costanzo, A.; Saccoccia, F.; Ruberti, G.; Jung, M.; Altucci, L.; Gemma, S.; Butini, S.; Christianson, D. W.; Campiani, G. Spiroindoline-Capped Selective HDAC6 Inhibitors: Design, Synthesis, Structural Analysis, and Biological Evaluation. *ACS Med Chem Lett* **2020**, *11* (11), 2268–2276. https://doi.org/10.1021/acsmedchemlett.0c00395.

(30) Federico, S.; Khan, T.; Fontana, A.; Brogi, S.; Benedetti, R.; Sarno, F.; Carullo, G.; Pezzotta, A.; Saraswati, A. P.; Passaro, E.; Pozzetti, L.; Papa, A.; Relitti, N.; Gemma, S.; Butini, S.; Pistocchi, A.; Ramunno, A.; Vincenzi, F.; Varani, K.; Tatangelo, V.; Patrussi, L.; Baldari, C. T.; Saponara, S.; Gorelli, B.; Lamponi, S.; Valoti, M.; Saccoccia, F.; Giannaccari, M.; Ruberti, G.; Herp, D.; Jung, M.; Altucci, L.; Campiani, G. Azetidin-2-One-Based Small Molecules as Dual HHDAC6/HDAC8 Inhibitors: Investigation of Their Mechanism of Action and Impact of Dual Inhibition Profile on Cell Viability. *Eur J Med Chem* **2022**, *238*, 114409. https://doi.org/10.1016/J.EJMECH.2022.114409.

(31) Relitti, N.; Saraswati, A. P.; Chemi, G.; Brindisi, M.; Brogi, S.; Herp, D.; Schmidtkunz, K.; Saccoccia, F.; Ruberti, G.; Ulivieri, C.; Vanni, F.; Sarno, F.; Altucci, L.; Lamponi, S.; Jung, M.; Gemma, S.; Butini, S.; Campiani, G. Novel Quinolone-Based Potent and Selective HDAC6 Inhibitors: Synthesis, Molecular Modeling Studies and Biological Investigation. *Eur J Med Chem* **2020**, *90* (xxxx), 112998. https://doi.org/10.1016/j.ejmech.2020.112998.

(32) Papa, A.; Cursaro, I.; Pozzetti, L.; Contri, C.; Cappello, M.; Pasquini, S.; Carullo, G.; Ramunno, A.; Gemma, S.; Varani, K.; Butini, S.; Campiani, G.; Vincenzi, F. Pioneering First-in-Class FAAH-HDAC Inhibitors as Potential Multitarget Neuroprotective Agents. *Arch Pharm (Weinheim)* **2023**, *356* (12), 2300410. https://doi.org/10.1002/ARDP.202300410.

(33) Safrygin, A.; Dar'in, D.; Bakulina, O.; Krasavin, M. Synthesis of Spirocyclic Tetrahydroisoquinolines (SpiroTHIQs) via the Castagnoli-Cushman Reaction. *Tetrahedron Lett* **2020**, *61* (42), 152408. https://doi.org/10.1016/J.TETLET.2020.152408.

(34) Gemma, S.; Camodeca, C.; Sanna Coccone, S.; Joshi, B. P.; Bernetti, M.; Moretti, V.; Brogi, S.; De Marcos, M. C. B.; Savini, L.; Taramelli, D.; Basilico, N.; Parapini, S.; Rottmann, M.; Brun, R.; Lamponi, S.; Caccia, S.; Guiso, G.; Summers, R. L.; Martin, R. E.; Saponara, S.; Gorelli, B.; Novellino, E.; Campiani, G.; Butini, S. Optimization of 4-Aminoquinoline/Clotrimazole-Based Hybrid Antimalarials: Further Structure-Activity Relationships, in Vivo Studies, and Preliminary Toxicity Profiling. *J Med Chem* **2012**, *55* (15), 6948–6957. https://doi.org/10.1021/JM300802S/SUPPL_FILE/JM300802S_SI_001.PDF.

(35) Mazzotta, S.; Berastegui-Cabrera, J.; Carullo, G.; Vega-Holm, M.; Carretero-Ledesma, M.; Mendolia, L.; Aiello, F.; Iglesias-Guerra, F.; Pachón, J.; Vega-Pérez, J. M.; Sánchez-Céspedes, J. Serinol-Based Benzoic Acid Esters as New Scaffolds for the Development of Adenovirus Infection Inhibitors: Design, Synthesis, and In Vitro Biological Evaluation. *ACS Infect Dis* **2021**, *7* (6), 1433–1444. https://doi.org/10.1021/acsinfecdis.0c00515.

(36) Federico, S.; Khan, T.; Fontana, A.; Brogi, S.; Benedetti, R.; Sarno, F.; Carullo, G.; Pezzotta, A.; Saraswati, A. P.; Passaro, E.; Pozzetti, L.; Papa, A.; Relitti, N.; Gemma, S.; Butini, S.; Pistocchi, A.; Ramunno, A.; Vincenzi, F.; Varani, K.; Tatangelo, V.; Patrussi, L.; Baldari, C. T.; Saponara, S.; Gorelli, B.; Lamponi, S.; Valoti, M.; Saccoccia, F.; Giannaccari, M.; Ruberti, G.; Herp, D.; Jung, M.; Altucci, L.; Campiani, G. Azetidin-2-One-Based Small Molecules as Dual HHDAC6/HDAC8 Inhibitors: Investigation of Their Mechanism of Action and Impact of Dual Inhibition Profile on Cell Viability. *Eur J Med Chem* **2022**, *238*. https://doi.org/10.1016/j.ejmech.2022.114409.

(37) Carullo, G.; Rossi, S.; Giudice, V.; Pezzotta, A.; Chianese, U.; Scala, P.; Carbone, S.; Fontana, A.; Panzeca, G.; Pasquini, S.; Contri, C.; Gemma, S.; Ramunno, A.; Saponara, S.; Galvani, F.; Lodola, A.; Mor, M.; Benedetti, R.; Selleri, C.; Varani, K.; Butini, S.; Altucci, L.; Vincenzi, F.; Pistocchi, A.; Campiani, G. Development of Epigenetic Modifiers with Therapeutic Potential in FMS-Related Tyrosine Kinase 3/Internal Tandem Duplication (FLT3/ITD) Acute Myeloid Leukemia and Other Blood Malignancies. *ACS Pharmacol Transl Sci* **2024**. https://doi.org/10.1021/ACSPTSCI.4C00208/SUPPL_FILE/PT4C00208_SI_001.PDF.

(38) Carullo, G.; Orsini, N.; Piano, I.; Pozzetti, L.; Papa, A.; Fontana, A.; Napoli, D.; Corsi, F.; Marco, B. Di; Galante, A.; Marotta, L.; Panzeca, G.; O'Brien, J.; Sanchez, A. G.; Doherty, H.; Mahon, N.; Clarke, L.; Contri, C.; Pasquini, S.; Gorelli, B.; Saponara, S.; Valoti, M.; Vincenzi, F.; Varani, K.; Ramunno, A.; Brogi, S.; Butini, S.; Gemma, S.; Kennedy, B. N.; Gargini, C.; Strettoi, E.; Campiani, G. Targeting Relevant HDACs to Support the Survival of Cone Photoreceptors in Inherited Retinal Diseases: Identification of a Potent Pharmacological Tool with In Vitro and In Vivo Efficacy. *J Med Chem* **2024**. https://doi.org/10.1021/ACS.JMEDCHEM.4C00477/SUPPL_FILE/JM4C00477_SI_002.PDF.

(39) Papa, A.; Pasquini, S.; Galvani, F.; Cammarota, M.; Contri, C.; Carullo, G.; Gemma, S.; Ramunno, A.; Lamponi, S.; Gorelli, B.; Saponara, S.; Varani, K.; Mor, M.; Campiani, G.; Boscia, F.; Vincenzi, F.; Lodola, A.; Butini, S. Development of Potent and Selective FAAH Inhibitors with Improved Drug-like Properties as Potential Tools to Treat Neuroinflammatory Conditions. *Eur J Med Chem* **2023**, *246*. https://doi.org/10.1016/j.ejmech.2022.114952.

(40) Grunewald, G. L.; Seim, M. R.; Lu, J.; Makboul, M.; Criscione, K. R. Application of the Goldilocks Effect to the Design of Potent and Selective Inhibitors of Phenylethanolamine N-Methyltransferase: Balancing PKa and Steric Effects in the Optimization of 3-Methyl-1,2,3,4-Tetrahydroisoquinoline Inhibitors by β-Fluorination. *J Med Chem* **2006**, *49* (10), 2939–2952. https://doi.org/10.1021/JM051262K/SUPPL_FILE/JM051262KSI20060315_024509.PDF.

(41) Porter, N. J.; Mahendran, A.; Breslow, R.; Christianson, D. W. Unusual Zinc-Binding Mode of HDAC6-Selective Hydroxamate Inhibitors. *Proc Natl Acad Sci U S A* **2017**, *114* (51), 13459–13464. https://doi.org/10.1073/PNAS.1718823114.

(42) Hai, Y.; Christianson, D. W. Histone Deacetylase 6 Structure and Molecular Basis of Catalysis and Inhibition. *Nat Chem Biol* **2016**, *12* (9), 741–747. https://doi.org/10.1038/nchembio.2134.

(43) De Vivo, M.; Masetti, M.; Bottegoni, G.; Cavalli, A. Role of Molecular Dynamics and Related Methods in Drug Discovery. *J Med Chem* **2016**, *59* (9), 4035–4061. https://doi.org/10.1021/ACS.JMEDCHEM.5B01684/ASSET/IMAGES/LARGE/JM-2015-016843_0006.JPEG.

(44) Carullo, G.; Bottoni, L.; Pasquini, S.; Papa, A.; Contri, C.; Brogi, S.; Calderone, V.; Orlandini, M.; Gemma, S.; Varani, K.; Butini, S.; Galvagni, F.; Vincenzi, F.; Campiani, G. Synthesis of Unsymmetrical Squaramides as Allosteric GSK-3β Inhibitors Promoting β-Catenin-Mediated Transcription of TCF/LEF in Retinal Pigment Epithelial Cells. *ChemMedChem* **2022**, *17* (24). https://doi.org/10.1002/CMDC.202200456.

(45) Vallone, A.; D'Alessandro, S.; Brogi, S.; Brindisi, M.; Chemi, G.; Alfano, G.; Lamponi, S.; Lee, S. G.; Jez, J. M.; Koolen, K. J. M.; Dechering, K. J.; Saponara, S.; Fusi, F.; Gorelli, B.; Taramelli, D.; Parapini, S.; Caldelari, R.; Campiani, G.; Gemma, S.; Butini, S. Antimalarial Agents against Both Sexual and Asexual Parasites Stages: Structure-Activity Relationships and Biological Studies of the Malaria Box Compound 1-[5-(4-Bromo-2-Chlorophenyl)Furan-2-Yl]-N-[(Piperidin-4-Yl)Methyl]Methanamine (MMV019918) and Analog. *Eur J Med Chem* **2018**, *150*, 698–718. https://doi.org/https://doi.org/10.1016/j.ejmech.2018.03.024.

(46) Carullo, G.; Saponara, S.; Ahmed, A.; Gorelli, B.; Mazzotta, S.; Trezza, A.; Gianibbi, B.; Campiani, G.; Fusi, F.; Aiello, F. Novel Labdane Diterpenes-Based Synthetic Derivatives: Identification of a Bifunctional Vasodilator That Inhibits CaV1.2 and Stimulates KCa1.1 Channels. *Mar Drugs* **2022**, *20* (8), 515. https://doi.org/10.3390/md20080515.

(47) Brindisi, M.; Butini, S.; Franceschini, S.; Brogi, S.; Trotta, F.; Ros, S.; Cagnotto, A.; Salmona, M.; Casagni, A.; Andreassi, M.; Saponara, S.; Gorelli, B.; Weikop, P.; Mikkelsen, J. D.; Scheel-kruger, J.; Sandager-nielsen, K.; Novellino, E.; Campiani, G.; Gemma, S.; Moro, A. Targeting Dopamine D 3 and Serotonin 5 - HT. **2014**.

(48) Saito, S, Zhuang, Y, Shan, B, Danchuk, S, Luo, F, Korfei, M, Guenther, A, Lasky, JA. Tubastatin Ameliorates Pulmonary Fibrosis by Targeting the TGFβ-PI3K-Akt Pathway. *PLoS One* **2017**, *12* (10), e0186615.

(49) Korfei, M.; Stelmaszek, D.; MacKenzie, B. A.; Skwarna, S.; Chillappagari, S.; Bach, A. C.; Ruppert, C.; Saito, S.; Mahavadi, P.; Klepetko, W.; Fink, L.; Seeger, W.; Lasky, J. A.; Pullamsetti, S. S.; Krämer, O. H.; Guenther, A. *Comparison of the Antifibrotic Effects of the Pan-Histone Deacetylase-Inhibitor Panobinostat versus the IPF-Drug Pirfenidone in Fibroblasts from Patients with Idiopathic Pulmonary Fibrosis*; 2018; Vol. 13. https://doi.org/10.1371/journal.pone.0207915.

(50) Sun, K. H.; Chang, Y.; Reed, N. I.; Sheppard, D. α-Smooth Muscle Actin Is an Inconsistent Marker of Fibroblasts Responsible for Force-Dependent TGFβ Activation or Collagen

Production across Multiple Models of Organ Fibrosis. *Am J Physiol Lung Cell Mol Physiol* **2016**, *310* (9), L824–L836. https://doi.org/10.1152/AJPLUNG.00350.2015.

(51) Zhao, W.; Wang, X.; Sun, K. H.; Zhou, L. α-Smooth Muscle Actin Is Not a Marker of Fibrogenic Cell Activity in Skeletal Muscle Fibrosis. *PLoS One* **2018**, *13* (1), e0191031. https://doi.org/10.1371/JOURNAL.PONE.0191031.

(52) Surolia, R.; Li, F. J.; Wang, Z.; Li, H.; Dsouza, K.; Thomas, V.; Mirov, S.; Pérez-Sala, D.; Athar, M.; Thannickal, V. J.; Antony, V. B. Vimentin Intermediate Filament Assembly Regulates Fibroblast Invasion in Fibrogenic Lung Injury. *JCI Insight* **2019**, *4* (7). https://doi.org/10.1172/JCI.INSIGHT.123253.

(53) Ma, J.; Li, G.; Wang, H.; Mo, C. Comprehensive Review of Potential Drugs with Anti-Pulmonary Fibrosis Properties. *Biomedicine & Pharmacotherapy* **2024**, *173*, 116282. https://doi.org/10.1016/J.BIOPHA.2024.116282.

(54) Libra, A.; Sciacca, E.; Muscato, G.; Sambataro, G.; Spicuzza, L.; Vancheri, C. Highlights on Future Treatments of IPF: Clues and Pitfalls. *International Journal of Molecular Sciences 2024, Vol. 25, Page 8392* **2024**, *25* (15), 8392. https://doi.org/10.3390/IJMS25158392.

(55) Cheng, H. P.; Jiang, S. H.; Cai, J.; Luo, Z. Q.; Li, X. H.; Feng, D. D. Histone Deacetylases: Potential Therapeutic Targets for Idiopathic Pulmonary Fibrosis. *Front Cell Dev Biol* **2024**, *12*, 1426508. https://doi.org/10.3389/FCELL.2024.1426508/BIBTEX.

(56) Rossi, S.; Tatangelo, V.; Dichiara, M.; Butini, S.; Gemma, S.; Brogi, S.; Pasquini, S.; Cappello, M.; Vincenzi, F.; Varani, K.; Lopresti, L.; Malchiodi, M.; Carrara, C.; Gozzetti, A.; Bocchia, M.; Marotta, G.; Patrussi, L.; Carullo, G.; Baldari, C. T.; Campiani, G. A Novel Potent Class I HDAC Inhibitor Reverses the STAT4/P66Shc Apoptotic Defect in B Cells from Chronic Lymphocytic Leukemia Patients. *Biomedicine & Pharmacotherapy* **2024**, *174*, 116537. https://doi.org/10.1016/J.BIOPHA.2024.116537.

(57) Carullo, G.; Borghini, F.; Fusi, F.; Saponara, S.; Fontana, A.; Pozzetti, L.; Fedeli, R.; Panti, A.; Gorelli, B.; Aquino, G.; Basilicata, M. G.; Pepe, G.; Campiglia, P.; Biagiotti, S.; Gemma, S.; Butini, S.; Pianezze, S.; Loppi, S.; Cavaglioni, A.; Perini, M.; Campiani, G. Traceability and Authentication in Agri-Food Production: A Multivariate Approach to the Characterization of the Italian Food Excellence Elephant Garlic (Allium Ampeloprasum L.), a Vasoactive Nutraceutical. *Food Chem* **2024**, *444*, 138684. https://doi.org/10.1016/J.FOODCHEM.2024.138684.

Supporting Information

The Supporting Information is available free of charge at XXXXX

Chemistry section

Synthesis and characterization of compounds **5a**-**o**; Preparation of the model and docking studies; Molecular Dynamics simulations for compound **5n**.

Biological section

HDAC inhibition assays; Cell culture; Cell viability assays; Total protein extraction; Histone extraction; Western Blot analysis; Zebrafish model; Zebrafish treatments; Animals; Isolated Rat Heart Preparation and Perfusion; Ex vivo studies; Flow cytometric analysis; HDAC Activity Assay; Statistical analysis.

Figure S1. A) Analysis of the interatomic distance between the NH of the ureidic group of 5n and the oxygen atom of Ser568 side chain throughout 250 ns-long MD simulations, performed starting from three different docking poses of the ligand. B) Frequency distribution of the water-mediated polar contact between the side chain of His651 and ureidic functional group of 5n (the frequency distribution is calculated over 2500 frames collected throughout each 250 ns-long MD simulation. A value equal to 0 or 1 would correspond to the 0% or 100%, respectively, of MD simulation frames featuring a water molecule bridging 5n and His651).

Figure S2. Cell Viability in U2OS was assessed by MTT assay by testing **5n**, **5m**, **5k**, and **5l** at final concentrations of 1 μM, 5 μM, 10 μM, 25 μM, 50 μM for 24, 48 and 72 h. SAHA was used at 5 μM, Tubastatin A and PCI at 10 μM.

Table S1. Solubility and chemical stability of compounds **5k,l**-**n**.

Table S2. Effects of **5n** on HR, RR, PQ, QRS, QT, and QTc in Langendorff Perfused Rat Hearts

Figure S3. Flow cytometric gating strategy applied to cell lines

Spectroscopic data and HPLC purity of compounds **5k**, **5l**, **5m**, and **5n**

For Table of Contents Use Only

Spirotetrahydroisoquinoline-based histone deacetylase inhibitors as new anti-fibrotic agents: biological evaluation in human fibroblasts from bronchoalveolar lavages of idiopathic pulmonary fibrosis patients

Anna Fontana[γ], Laura Bergantini[ε], Gabriele Carullo[γ], Laura Scalvini[φ], Miriana D'Alessandro[ε], Chiara Papulino[ω], Paolo Cameli[ε], Sara Gangi[ε], Fabrizio Vincenzi[§], Katia Varani[§], Chiara Contri[§], Silvia Pasquini[θ], Anna Pistocchi[Ψ], Alex Pezzotta[Ψ], Sabrina Carbone[Ψ], Simona Saponara[μ], Sandra Gemma[γ,*], Lucia Altucci[ω,Θ,ϱ], Rosaria Benedetti[ω], Alessio Lodola[φ], Marco Mor[φ,ζ], Elena Bargagli[ε], Stefania Butini[γ], Giuseppe Campiani[γ,*]

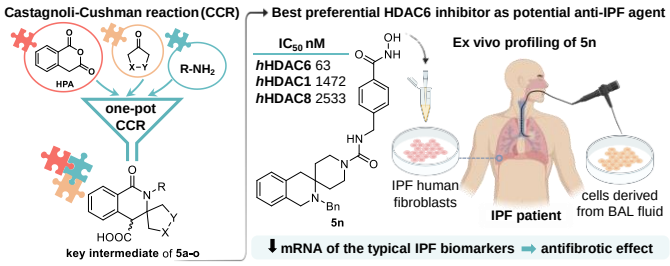

Synopsis

The one-pot Castagnoli-Cushman protocol furnished scaffolds for the development of inhibitors preferentially targeting HDAC6. The most promising candidate **5n**, was tested in two different *ex vivo* models of the fatal disease idiopathic pulmonary fibrosis, proving to be able to successfully revert fibrotic phenotype at very low doses.